Synthetic Lethality Screen Identifies a Novel Yeast Myosin I Gene (*MYO5*): Myosin I Proteins Are Required for Polarization of the Actin Cytoskeleton

Holly V. Goodson,* Blake L. Anderson,§ Hans M. Warrick,* Liza A. Pon,‡ and James A. Spudich*

*Departments of Biochemistry and Developmental Biology, Stanford University, Stanford, CA 94305;‡Department of Cell Biology, and §Department of Pathology, Columbia University College of Physicians and Surgeons, New York 10032

Abstract. The organization of the actin cytoskeleton plays a critical role in cell physiology in motile and nonmotile organisms. Nonetheless, the function of the actin based motor molecules, members of the myosin superfamily, is not well understood. Deletion of *MYO3*, a yeast gene encoding a "classic" myosin I, has no detectable phenotype. We used a synthetic lethality screen to uncover genes whose functions might overlap with those of *MYO3* and identified a second yeast myosin I gene, *MYO5*. *MYO5* shows 86 and 62% identity to *MYO3* across the motor and non-motor regions. Both genes contain an amino terminal motor domain, a neck region containing two IQ motifs, and a tail domain consisting of a positively charged region, a proline-rich region containing sequences implicated in ATP-insensitive actin binding, and an SH3 domain. Although *myo5* deletion mutants have no detectable phenotype, yeast strains deleted for both *MYO3* and *MYO5* have severe defects in growth and actin cytoskeletal organization. Double deletion mutants also display phenotypes associated with actin disorganization including accumulation of intracellular membranes and vesicles, cell rounding, random bud site selection, sensitivity to high osmotic strength, and low pH as well as defects in chitin and cell wall deposition, invertase secretion, and fluid phase endocytosis. Indirect immunofluorescence studies using epitope-tagged Myo5p indicate that Myo5p is localized at actin patches. These results indicate that *MYO3* and *MYO5* encode classical myosin I proteins with overlapping functions and suggest a role for Myo3p and Myo5p in organization of the actin cytoskeleton of *Saccharomyces cerevisiae.*

THE myosin superfamily of molecular motors encompasses at least eleven different classes of proteins (Cheney et al., 1993; Sellers and Goodson, 1995). While the conventional myosin (myosin II) has been studied in great detail in both muscle and nonmuscle cells, comparatively little is known about most unconventional myosin proteins. Myosin I proteins were the first unconventional myosins discovered (Pollard and Korn, 1973; Hammer et al., 1986). Members of the myosin I class have now been identified in phylogenetically diverse organisms (for review see Sellers and Goodson, 1995), suggesting that they are ubiquitous, ancient proteins with a central role in eukaryotic cell biology.

Myosin I proteins can be divided into at least two subclasses based on homologies in motor and tail domains (Hasson and Mooseker, 1995). "Classic" myosin I proteins have been found in fungi, ameboid cells, and metazoans (for review, see Sellers and Goodson, 1995). These proteins possess tail domains containing a positively charged region implicated in membrane binding, a proline-rich region, and an SH3 domain (for review, see Hammer, 1991). The proline-rich region contains sequences implicated in ATP-insensitive actin binding (Lynch et al., 1986; Doberstein and Pollard, 1992; Jung and Hammer, 1994; Rosenfeld and Rener, 1994). Between the motor and tail domains is a "neck" region containing one or two "IQ" motifs, sequences expected to bind to calmodulin or calmodulin-related myosin light chains (Cheney and Mooseker, 1992). In contrast, the brush border myosin I's and related proteins have tails with only the putative membrane binding region and necks with 3–6 IQ motifs. Proteins clearly related to the brush border myosins have been found only in metazoans, although similar proteins exist in ameboid cells (reviewed by Sellers and Goodson, 1995).

The function of myosin I proteins is not well understood. One model proposes that myosin I proteins bind to both microfilaments and organelles and use the energy of ATP hydrolysis to drive organelle movement along actin tracks (Adams and Pollard, 1989). Alternatively, myosin I proteins could act to connect the plasma membrane to the

Address all correspondence to Dr. Liza A. Pon, Department of Anatomy and Cell Biology, Columbia University P&S 12-425, 630 W. 168th Street, New York, NY 10032. Tel: (212) 305-1947. Fax: (212) 305-3970.

H.V. Goodson and B.L. Anderson contributed equally to this work and are first co-authors.

actin cytoskeleton and drive movements of the cytoskeleton against the membrane. A classic myosin-I–specific variation of this model proposes that the second, ATP-insensitive, actin-binding site in the tail could be used to cross-link actin filaments and allow myosin-I to drive F-actin sliding on actin filaments, thus altering actin organization at the membrane interface.

Experimental observations obtained thus far are consistent with all of these proposed functions. In *Dictyostelium*, myosin I proteins have been implicated in cell motility, phagocytosis, and pseudopod formation (Jung and Hammer, 1990; Wessels et al., 1991; Jung et al., 1993; Titus et al., 1993). Syringe loading of inhibitory antibodies indicates that one myosin I protein, *Acanthamoeba* IC, is essential for the function of the *Acanthamoeba* contractile vacuole (Doberstein et al., 1993). Finally, recent studies in *Aspergillus nidulans* indicate that the MyoA gene encodes an essential myosin I required for secretion and polarized growth (McGoldrick et al., 1995).

Previous studies identified in *Saccharomyces cerevisiae* a gene that encodes a classic myosin I protein, *MYO3*. Deletion of this gene had no discernible phenotypic effects under laboratory conditions, presumably for reasons of functional redundancy (Goodson and Spudich, 1995). However, deletion of *MYO3* in combination with mutations of other known yeast myosin genes (*MYO1*, a myosin II, *MYO2*, a myosin V, or *MYO4*, a myosin V) has no detectable effect (Goodson and Spudich, 1995; Haarer et al., 1994; Lillie, S.L., and S.S. Brown, unpublished results). These findings indicate that the redundant protein is not one of the known yeast myosins. We used a genetic screen to identify mutations that create a requirement for *MYO3*. This strategy, termed a synthetic lethality screen, has been useful for identification of genes that are involved in a common process (for example, see Bender and Pringle, 1991). We present results of such a screen and demonstrate that it identifies a new yeast myosin I gene, *MYO5*. We demonstrate that yeast strains deleted for both *MYO3* and *MYO5* have a severe defect in growth, actin polarization, and actin-dependent processes including secretion, endocytosis, and polarity establishment. We suggest that the primary defect in the mutants bearing classic myosin I deletions is abnormal polarization of the actin cytoskeleton.

Materials and Methods

Yeast And Bacterial Manipulations

Yeast manipulations including cell culture, transformation, and tetrad analysis were carried out according to Guthrie and Fink (1991). Bacterial manipulations were carried out according to Sambrook et al. (1989).

Synthetic Lethality Screen

myo5 mutants were isolated using a synthetic lethal strategy based on selection against the *URA3* gene. A yeast strain (HA10-1c) containing a deletion of *MYO3* (Table I) was transformed with a centromere-based, pRS316-derived plasmid (P316SRMYO3) which contains the *URA3* marker and the full coding region of *MYO3* (Sikorski and Hieter, 1989). Transformants were mutagenized with ethylmethane sulfonate (EMS)[1] until only ~25% of the cells were viable (Lawrence, 1991). Transformants were replica plated to uracil-free plates and to plates containing 5-fluoroorotic acid (5-FOA). Since 5-FOA kills cells expressing the *URA3* gene, this method distinguishes colonies that require the *MYO3*-containing plasmid from those that do not. From 10,000 mutagenized colonies screened, ~120 grew poorly on unbuffered 5-FOA containing media after incubation at 30°C. Three of these strains (C11, 37, and D2) uniformly maintained the *URA3* marker under nonselective conditions and were kept for further examination.

Cloning and Sequence Analysis

The *MYO5* gene was cloned by complementation of mutant 37 with a plasmid library. The library consisted of genomic yeast DNA partially digested with Sau3A and sub-cloned into a centromere-based, *LEU2*-containing shuttle vector derived from YCP50 (Christianson et al., 1992; American Type Culture Collection, Rockville, MD; ATCC No. 77162). Of ~12,000 Leu+ transformants, 46 colonies were no longer dependent upon retention of p316SR*MYO3* (the *MYO3*-containing plasmid marked by *URA3*) as assayed by survival of these colonies at 30°C on solid, unbuffered minimal medium (SD) containing 5-FOA. Library plasmids were isolated from 40 of these colonies (Ward, 1990). 29 contained the *MYO3* gene and 11 contained a different set of overlapping inserts which conferred 5-FOA resistance to synthetic lethal mutants. The DNA sequence of this insert was determined as described previously (Goodson and Spudich, 1995). Sequence analysis of the region which conferred FOA resistance revealed a new myosin I gene, *MYO5*. Similar results were obtained by complementation of mutant C11 with the same library. Sequences were analyzed with the GCG Package (Genetics Computer Group, Inc., Madison, WI).

Disruption of MYO5

A strain of yeast missing all of the *MYO5* coding sequence (as well as 95 bases of 5′ noncoding sequence) was created by a "delta deletion" (Sikorski and Hieter, 1989). 3′ and 5′ noncoding sequence of the *MYO5* locus were inserted into the integrating plasmid pRS304 in a direct orientation to create the plasmid p304KO3 (see Fig. 1). p304KO3 was linearized with SpeI to cut between the 3′ and 5′ inserts and transformed into the diploid yeast strains CRY3 and HA20. Southern blot analysis revealed that sequences between the 5′ and 3′ inserts on one chromosome of the transformant were replaced by the plasmid DNA. Haploid strains bearing the *MYO5* deletion were isolated by tetrad dissection. The Trp+ phenotype marking the deletion segregated 2:2 in both the CRY3 and HA20 transformants and was tightly linked to growth defects in the HA20 transformants (data not shown).

Construction of Epitope-tagged Myo5p

Myo5p was epitope tagged by insertion of three copies of the 11 amino acid epitope from human c-myc (Evan et al., 1985) at the extreme COOH terminus of the protein. To do so, the stop codon of *MYO5* was replaced with a BamHI site using PCR. The 3′ end of the modified *MYO5* gene was then excised using BamHI and BstEII. This product was ligated to a 4.8-kb SpeI-BstEII fragment which consists of the remainder of the *MYO5* gene and 1.8 kb of its 5′ noncoding region containing the *MYO5* promoter region. The ligated products were digested with SpeI and BamHI, and subcloned into the KS Bluescript vector (Stratagene, La Jolla, CA). Three copies of the myc tag coding sequence were excised from the pKK-1 plasmid with BamHI and inserted in frame at the BamHI site at the 3′ end of the *MYO5* gene. An NheI linker (New England Biolabs Inc., Beverly, MA) containing a stop codon in all three reading frames was inserted immediately downstream from the myc tag. The entire construct was excised with SacI and XhoI and sub-cloned into the centromere-based yeast shuttle vector, pRS-Y2, a derivative of pRS316 which contains the multiple cloning site of pYES2 (InVitrogen, San Diego, CA). This construct is referred to as pRS-Y2-myc-*MYO5*. A construct containing untagged *MYO5* and 1.8 kb of its 5′ noncoding region (pRS-Y2-*MYO5*) was produced using a similar approach.

Light Microscopy

Actin cytoskeletal structure and chitin deposition were visualized using rhodamine-phalloidin, a rabbit polyclonal antibody raised against yeast actin (Drubin et al., 1988), and Calcofluor (Sigma Chemical Co., St. Louis, MO) according to published procedures (Adams et al., 1991; Pringle et al. 1991). Cell viability was determined using the FUN-1 cell stain (Molecular

1. *Abbreviations used in this paper*: 5-FOA, 5-fluoroorotic acid; EMS, ethylmethane sulfonate; SH3, Src Homology 3.

Table I. Yeast Strains Used in This Study

Strain	Genotype	Reference
MSY106	MATa/MATα, *his4-619/his4-619*	Smith et al., 1995
MSY202	MATa/MATα, *his4-619/his4-619, act1-3/act1-3*	Smith et al., 1995
CRY3	MATa/MATα, *can1-100/can1-100, ade2-1/ade2-1, his3-11/his3-11, leu2-3,112/leu2-3,112, ura3-1/ura3-1*	Goodson and Spudich, 1995
HA20	MATa/MATα, *can1-100/can1-100, ade2-1/ade2-1, his3-11/his3-11, leu2-3,112/leu2-3,112, trp1-1/trp1-1, ura3-1/ura3-1, myo3::HIS/myo3::HIS3*	Goodson and Spudich, 1995
HA31	*MATa/MATα, can1-100/can1-100, ade2-1/ade2-1, his3-11,-15/his3-11,-15, leu2-3,-112/leu2-3,-112, trp1-1/trp1-1, ura3-1/ura3-1, myo3::HIS3/myo3::HIS3 MYO5/myo5::TRP1*	this study
HA10-1b	MATα, *can1-100, ade2-1, his3-11, leu2-3,112, ura3-1, trp1-1*	this study
HA10-1c	MATa, *can1-100, ade2-1, his3-11, leu2-3,112, ura3-1, trp1-1, myo3::HIS3*	this study
HA51-1a	MATα, *can1-100, ade2-1, his3-11, leu2-3,112, ura3-1, trp1-1, myo5::TRP1*	this study
HA31-9a	MATα, *can1-100/, ade2-1, his3-11, leu2-3,112, ura3-1, trp1-1, myo3:: HIS3*	this study
HA31-9b	MATα, *can1-100/, ade2-1, his3-11, leu2-3,112, ura3-1, trp1-1, myo3:: HIS3, myo5::TRP1*	this study
HA31-9c	MATa, *can1-100/, ade2-1, his3-11, leu2-3,112, ura3-1, trp1-1, myo3:: HIS3, myo5::TRP1*	this study
HA31-9d	MATa, *can1-100/-, ade2-1, his3-11, leu2-3,112, ura3-1, trp1-1, myo3:: HIS3*	this study

Probes, Eugene, OR) according to manufacturer's instructions. Other methods (fixation, mounting, DAPI staining) were as described by Pringle et al. (1991). Photomicroscopy was performed on a Leitz Dialux microscope using a 100× (NA 1.4) objective (Rockleigh, NJ). Images were collected using a cooled CCD camera (model # Star-1; Photometrics, Tucson, AZ). Light output from the 100W Mercury Arc lamp was controlled using a shutter driver (model # Uniblitz D122; Vincent Associates, Rochester, NY) and attenuated using neutral density filters (Omega Optical Corporation, Brattleboro, VT). Image enhancement and analysis were performed on a Macintosh Quadra 800 computer (Cupertino, CA) using the public domain program NIH Image 1.55. Images were stored on a magnetic optical disk drive (Peripheral Land Inc., Fremont, CA).

Confocal images of cells were obtained with a laser scanning confocal microscope (model # MRC 600; Bio-Rad Microscience, Cambridge, MA) on a Zeiss Axiovert inverted microscope (Oberkochen, Germany) using a 63× (NA 1.4) Zeiss Plan-Apo infinity corrected objective. The illumination sources were the 488- and 514-nm lines from a 25-mW argon laser. Rhodamine-phalloidin was visualized with a 514-nm bandpass excitation filter, a 540-nm dichroic mirror and a 550-nm-long pass emission filter. Light was attenuated using neutral density filters in the excitation path. Each field of cells was sectioned three dimensionally by recording images from a series of 0.36 μm optical sections. Movement from one focal plane to the next was achieved using a stepper motor attached to the fine focus control of the microscope. Each optical section collected was the average of 15 scans at the confocal microscope's normal scan rate (1 frame/s). All images were processed and enhanced using the COMOS program (Bio-Rad Microscience, Cambridge, MA) and Adobe Photoshop 2.5 (Mountain View, CA).

Electron Microscopy

Preparation of samples for transmission electron microscopy was carried out according to Stevens (1977). Yeast were fixed by addition of glutaraldehyde (Sigma Chemical Co.) to growth medium to a final concentration of 5%. After incubation for 3 h at room temperature, cells were concentrated by centrifugation (10,000 *g*, 10 min, room temperature), and washed two times with 0.9% NaCl. Samples were resuspended in 4% $KMnO_4$ in 0.1 M Na-cacodylate, pH 7.4 (Electron Microscopy Sciences, Fort Washington, PA), and incubated at 4°C for 1 h with gentle rotation. After two washes with 0.9% NaCl, samples were resuspended in 2% uranyl acetate (Electron Microscopy Sciences) and incubated for 1 h at room temperature. Samples were washed three times, dehydrated in a graded series of ethanol solutions, infiltrated with propylene oxide for 10 min, and embedded in Epon-812 (Tousimis Research Co., Rockville, MD). Ultrathin sections were stained for 5 min with 1% lead citrate before viewing with a JEOL 1200 transmission electron microscope.

Invertase Secretion Assay

Secreted invertase was assayed as described (Goldstein and Lampen, 1975) in intact cells. Cells were grown to log phase in YEP media containing 2% glucose. Cultures were washed with YEP supplemented with 0.05% glucose, resuspended in this media, and incubated at 30°C with constant shaking. At the times indicated, cell densities were determined by OD_{600} measurements, and aliquots were removed from the culture. Cells were washed with ice cold 10 mM NaN_3, resuspended in 10 mM NaN_3, and stored on ice until all aliquots had been collected. A portion of each aliquot containing equal numbers of cells was added to 100 mM sodium acetate, pH 5.1, and 125 mM sucrose and incubated for 20 min at 37°C. Reactions were terminated by addition of 2.5 volumes 200 mM K_2HPO_4 and stored on ice. An aliquot from each terminated reaction was diluted with 4 volumes 200 mM K_2HPO_4 and boiled for 5 min to destroy invertase activity. The quantity of glucose in each sample was determined by addition of Glucostat reagent (100 mM KPi, pH 7.0, 20 μg/ml glucose oxidase, 2.5 μg/ml peroxidase, and 15 μg/ml *O*-diaisidine) and incubated at 37°C for 30 min. Color development was initiated by addition of one volume 6 M HCl and measured using a spectrophotometer (model DU-50; Beckman Instruments, Fullerton, CA) at 540 nm. Levels of glucose released were calculated by comparing absorption readings to a standard curve. Units of invertase activity are defined as micromoles of glucose released/min/10 mg cell (dry weight), assuming that 1 OD_{600} equals 0.19 mg cells/ml.

Lucifer Yellow Uptake Assay

The uptake of Lucifer yellow CH was performed according to Riezman (1985) with slight modifications. Cells were grown to log phase in YEP + 2% glucose and Lucifer yellow CH (Sigma Chemical Co.) was added to 4 mg/ml. After 60 min incubation at 30°C with constant agitation, cells were washed three times with ice cold 50 mM succinate, pH 5.0, 100 mM NaCl, 10 mM $MgCl_2$, 20 mM NaN_3. An aliquot of each sample was embedded in 0.8% low melt agarose on a glass slide and placed under a cover slip. Optical images were collected using the Leitz Dialux microscope as described above. Cells were scored as positive if the vacuole was clearly stained with Lucifer yellow.

Results

Synthetic Lethality Screen Identifies a New Yeast Myosin Gene, MYO5

Yeast deleted for the classic myosin I gene *MYO3* have no discernible defects, suggesting that another protein(s) has overlapping function with Myo3p (Goodson and Spudich, 1995). We conducted a synthetic lethality screen to identify such proteins. This genetic screen is based on the principle that yeast bearing mutations of either of two genes with overlapping function will remain viable. However, yeast mutated at both genes should have a defect in a basic biological function and are expected to die (Huffaker et al., 1987). Yeast carrying a chromosomal deletion of *MYO3* and a plasmid which contains a functional *MYO3* gene were mutagenized. Mutants which die if forced to lose the plasmid-borne *MYO3* were then identified by replica plating mutagenized colonies onto solid media containing 5-FOA. 5-FOA kills cells expressing the *URA3* gene, a nutritional marker present on the *MYO3*-containing plasmid. Therefore, cells that cannot lose the *MYO3*-containing plasmid will not grow on 5-FOA.

Three mutant strains (C11, 37, and D2) which were dependent on the *MYO3* plasmid were produced using this synthetic lethal screen. Dependence of these strains on *MYO3* was demonstrated in three ways. First, the mutants were transformed with a second plasmid (p314SR*MYO3*) containing the *MYO3* gene and a different selectable marker (*TRP1*). These strains were now able to grow on 5-FOA. In addition, plasmid loss assays indicate that these transformants could lose either *MYO3*-bearing plasmid, but not both. Second, mutants containing the *MYO3* gene under control of the galactose promoter displayed a galactose dependence for growth. Finally, a mutant form of p314SR*MYO3* containing a *MYO3* gene with a frame shift in the tail of *MYO3* (Fig. 1) will not support growth of the mutant. Backcrossing of the synthetic lethal mutants to the parent strain indicated that the mutations were recessive. Complementation tests indicated that all three synthetic lethal strains were in the same complementation group.

A new yeast myosin gene, *MYO5*, was cloned by complementation of the synthetic lethal phenotype. In complementary studies, this gene was also identified by PCR using degenerate, myosin I–specific oligonucleotides. The sequence of Myo5p (Fig. 2) shows that *MYO5* encodes a classic myosin I protein, like *MYO3*. It is 76.6% identical to *MYO3* over the whole protein, 87 and 62% identical in the head and tail, respectively. All of the motor and tail domains expected from a classic myosin I and identified in the tail of *MYO3* are also found in *MYO5*, including a basic (putative membrane-binding) region, an SH3 domain (Src Homology 3; see Hammer, 1991 for review), and a hyper-proline-rich region 10 amino acids before the SH3 domain (Goodson and Spudich, 1995). The region 100 amino acids amino terminal to the SH3 domain contains a higher proline content than that of the corresponding region in *MYO3* (25 vs 17% proline, respectively). In this respect, *MYO5* is more similar to other classical myosin I proteins than *MYO3*. Like *MYO3*, *MYO5* contains two IQ motifs, which are putative light chain binding sites (Cheney and Mooseker, 1992). The stretch of acidic residues followed

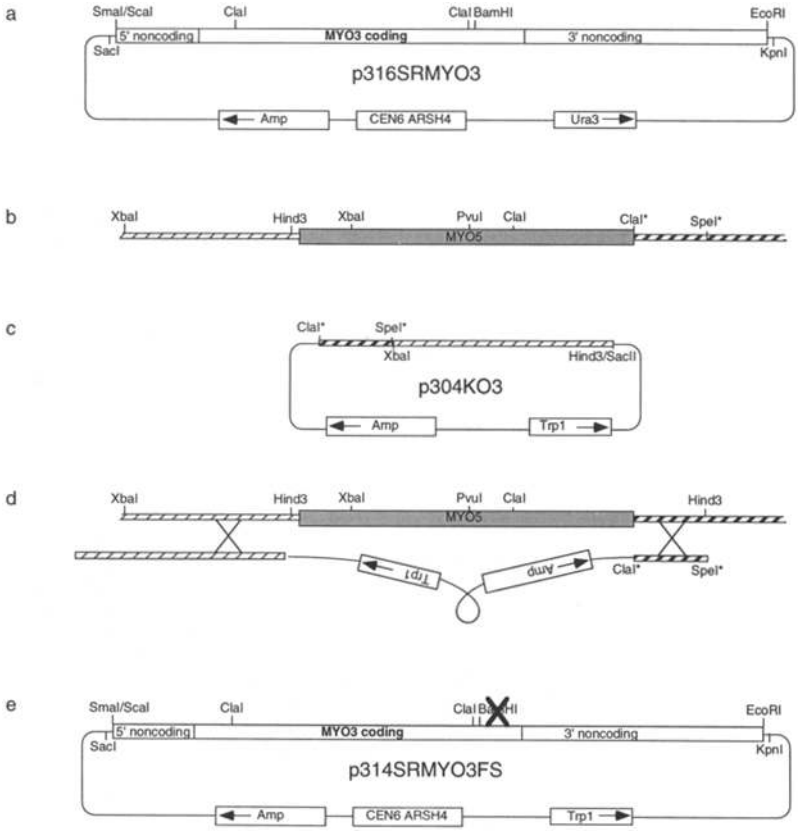

Figure 1. Plasmid construction and deletion of the *MYO5* gene. (*a*) *MYO3* expression plasmid p316SR*MYO3*; (*b*) map of chromosomal locus of *MYO5*; (*c*) deletion plasmid p304KO3; (*d*) schematic illustrating replacement of *MYO5* sequences with plasmid DNA; and (*e*) a mutant form of p314SR*MYO3* containing a *MYO3* gene with a frame shift in the tail of *MYO3* (p314SR*MYO3*FS). Restriction sites marked by "*" were introduced into *MYO5* by PCR subcloning and do not exist in the genomic version. The ClaI site in p304KO3 was placed at the stop codon. Nonmyosin regions of the plasmid are not drawn to scale. ▨, MYO5 5′ noncoding; ■, MYO5 coding region; ▨, MYO5 3′ noncoding; ——, = 1 kb.

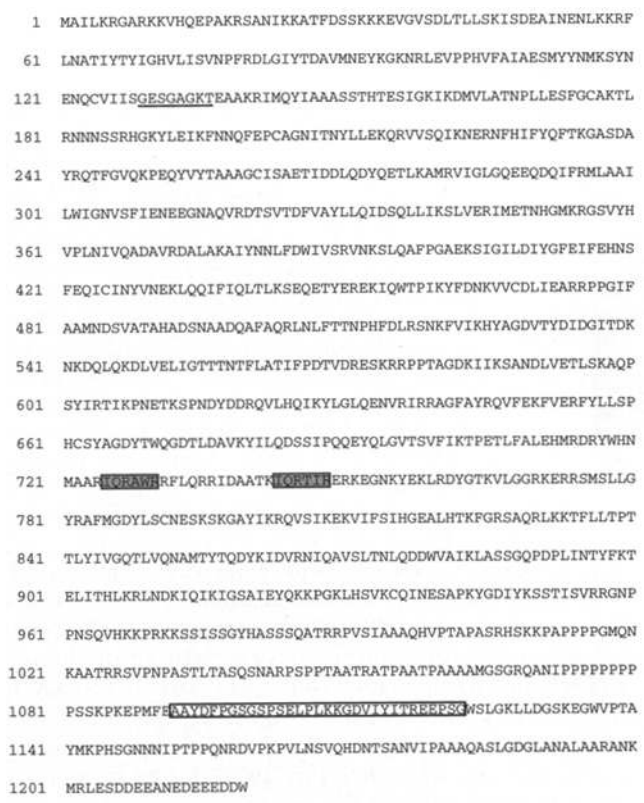

Figure 2. Derived amino acid sequence of Myo5p. This sequence is based on the DNA sequence of the *MYO5* gene. The *MYO5* DNA sequence shows 99% identity to sequence SC9718.08 obtained by the yeast genome sequencing project. The ATP binding site (*underlined*); IQ motifs (■); and SH3 motif (□).

by a tryptophan which is found at the end of both *MYO3* and *Aspergillus nidulans MYOA* (McGoldrick et al., 1995) is also found in *MYO5*. The functional significance of this sequence is not known. Sequence analysis of complementing genomic yeast DNA in regions adjacent to the *MYO5* gene indicate that this gene is located adjacent to *ILV2*, a gene required for amino acid biosynthesis previously mapped to chromosome XIII by classic genetic techniques (Falco and Dumas, 1985; Falco et al., 1985).

Mutants Bearing Deletions in MYO3 and MYO5 Display Slow Growth

MYO5 mutants obtained from the synthetic lethal screen were found after backcrossing to be viable under standard growth conditions (YPAD, pH 5.5, 30°C), but display severe growth defects. Therefore, the role of myosin I proteins in yeast cell function was studied in mutant yeast strains bearing deletions in one or both of the myosin I genes. Deletion of one myosin I gene has no significant effect on growth rates: *myo3Δ* and *myo5Δ* single mutants display doubling times equivalent to isogenic wild-type cells (Table II; Goodson and Spudich, 1995). In contrast, cells bearing deletions in *MYO3* and *MYO5* show greatly lengthened doubling times (Table II). Approximately 10% of the cells in an exponentially growing *myo3Δ,myo5Δ* mutant culture are inviable, as determined using the fungal viability dye Fun-1. However, mathematical modeling

Table II. Deletion of MYO3 and MYO5 Results in Slow Growth

Strain	Doubling time	SEM
	h	
HA10-1b (wt)	1.41	0.07
HA31-9a (*myo3Δ*)	1.34	0.05
HA51-1a (*myo5Δ*)	1.40	0.11
HA31-9c (*myo3Δ,myo5Δ*)	4.45	0.29
HA31-9c-pRS-Y2-*MYO5*	1.34	0.09
HA31-9c-pRS-Y2-myc-*MYO5*	1.35	0.09

Cultures of wild-type cells, mutants bearing single or double mutations in *MYO3* and *MYO5*, and a *myo3Δ,myo5Δ* mutant transformed with *MYO5* or myc-tagged *MYO5* on a centromeric plasmid (pRS-Y2) were grown to early log phase in rich medium (YPD) at 30°C. Aliquots were removed periodically from all cultures and the cells were sonicated briefly to disrupt cell clumps. Cell densities were determined by OD_{600} measurements and apparent doubling times were calculated.

of cell doubling indicates that this loss of cell viability contributes to but is not solely responsible for low growth rates (data not shown).

Double mutants are sensitive to cold (15°C) and elevated (37°C) temperature (Fig. 3). Double mutants did not accumulate at a particular point in the cell cycle after shift to cold (data not shown). During exponential growth at 30°C, they displayed a similar proportion of unbudded, small, medium, and large budded cells as the wild-type parental strain. Double mutants were defective for growth on solid rich media with high osmotic strength (0.75 M NaCl) or low pH (3.5). Tetrad analysis revealed that sensitivity to cold, elevated temperature, high osmotic strength, and low pH showed 2:2 segregation and segregated with deletion of both *MYO3* and *MYO5* (Fig. 3). Transformation of *myo3Δ,myo5Δ* mutants with a centromeric plasmid bearing *MYO5* under its own promoter restores the wild-type growth rates at 30°C (Table II), as well as growth at low and high temperatures, low pH, and high osmotic strength (data not shown). Thus, the low growth rate, sensitivity to cold, acidic pH, and high osmolarity observed in the *myo3Δ,myo5Δ* double mutants are due to the loss of both type I myosins.

To evaluate the localization of Myo5p in yeast (see below), we constructed epitope-tagged Myo5p by insertion of three copies of the myc tag (Evan et al., 1985) at the extreme COOH terminus of the protein. myc-tagged Myo5p was expressed in the *myo3Δ,myo5Δ* mutant using a low copy plasmid under control of the endogenous *MYO5* promoter. myc-tagged Myo5p restored normal growth rates in the myosin I double deletion mutant (Table II). This observation indicates that myc-tagged Myo5p is functional in living yeast.

Actin Patches and Cables Are Depolarized in the Double Mutant, myo3Δ,myo5Δ

The actin cytoskeleton of exponentially growing cultures of a wild-type haploid strain, a *myo5Δ* single mutant, and a *myo3Δ,myo5Δ* double deletion strain were visualized using rhodamine-phalloidin. The wild-type isogenic strain (HA10-1b) exhibits a typical polarized arrangement of actin patches (Fig. 4 *B*). 95% of wild-type cells with small- and medium-sized buds have actin patches exclusively in the buds. These actin patches appear to be invaginations in the plasma membrane which are invested with F-actin (Mulholland et al., 1994) and are thought to be involved in

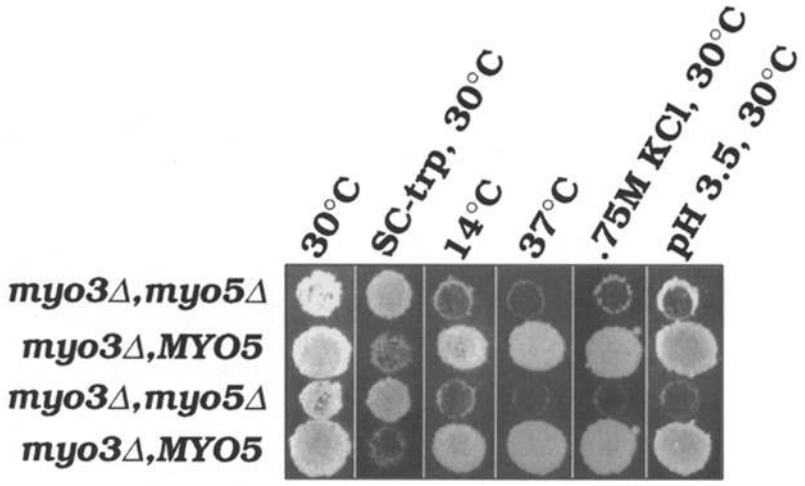

Figure 3. Growth characteristics of the *myo3Δ,myo5Δ* mutant. HA31, a diploid bearing deletion of both chromosomal copies of *MYO3* and of one chromosomal copy of *MYO5*, was sporulated. Haploid cells were isolated by tetrad dissection and were grown at 30°C on rich media (YPD). These cells were replica plated onto various media and grown at the temperatures shown. SC-trp was used to select for cells bearing disruption of *MYO5* and insertion of a *TRP1* marker. Sensitivity to cold, elevated temperatures and high osmotic strength were evaluated by growth on YPD at 14°C, 37°C and YPD supplemented with 0.75 M KCl at 30°C. A representative tetrad is shown.

late steps of secretion and/or early steps of endocytosis (Novick et al., 1981; Kübler and Riezman, 1993). Asymmetric arrangement of actin patches is lost in the double deletion strain (Fig. 4 *D*). The patches of cortical actin are distributed randomly over the surface of both mother and bud: polarization of actin patches exclusively in buds occurs in only 8% of the *myo3Δ,myo5Δ* mutants studied. This finding suggests that yeast myosin I proteins are required for polarized arrangement of actin patches. Consistent with this observation, proper cortical actin polarization can be fully restored by replacing *MYO5* on a low copy (centromere) plasmid under the control of its own promoter (Fig. 4 *F*).

Actin cables are the other major component of the yeast actin cytoskeleton. These cables are bundles of filamentous actin that are believed to function as tracks for polarized transport of organelles and vesicles from the mother cell to the bud (Novick and Botstein, 1985). In wild-type cells and in *myo5Δ* single mutants, actin cables are arranged in radial arrays that extend throughout the mother cell and converge at the bud neck (Fig. 4 *B*). The presence of brightly stained cortical actin patches in the mother cell of *myo3Δ,myo5Δ* mutants precluded resolution of actin cables by conventional fluorescence microscopy. However, these structures are readily detectable by confocal microscopy (Fig. 5). Some actin cables are observed to extend along the mother bud axis in the double mutant, as in the wild-type cell. However, many cables appear to be disorganized in the *myo3Δ,myo5Δ* double mutant: these cables are observed to extend across the mother cell rather than toward the bud neck. Our findings indicate that deletion of yeast myosin I genes results in loss of actin cable and patch polarization without qualitatively affecting the total staining intensity of these cytoskeletal elements.

Mitochondrial and Nuclear DNA Inheritance Occurs in the Double Mutant, myo3Δ,myo5Δ

Previous studies indicate that mutations in the actin-encoding *ACT1* gene result in defects in nuclear migration during cell division, aggregation of mitochondria, as well as defects in mitochondrial motility and inheritance (Novick and Botstein, 1985; Drubin et al., 1993; Lazzarino et al., 1994; Simon et al., 1995). The arrangement of nuclear and mitochondrial DNA in wild-type cells and in the *myo3Δ,myo5Δ* mutant was examined using the fluorescent DNA binding dye DAPI. In wild-type cells, DAPI staining reveals threads of mitochondria in both the mother cell and bud and accumulation of mitochondria in the bud tip (Fig. 4 *A*). Nuclear staining is quite prominent. In some cases, nuclei were observed to extend from a mother cell to the bud and were therefore fixed during transport of nuclei into a bud (Fig. 4 *A*).

In *myo3Δ,myo5Δ* mutant cells, mitochondria show low levels of aggregation but extended tubular mitochondrial structures are clearly visible (Fig. 4 *C*). Transformation of the *myo3Δ,myo5Δ* mutant strain with a centromeric plasmid containing *MYO5* fully rescues the wild-type mitochondrial phenotype (Fig. 4 *E*). Thus, deletion of both of these yeast myosin I genes causes some defects in mitochondrial spatial arrangement. However, transport of mitochondria into buds is not significantly affected in the double mutant. In mutant and wild-type strains, mitochondrial tubules were observed traversing the bud neck and accumulating at the bud tip. In addition, mitochondrial DNA was observed to be transferred to buds in greater than 90% of cells bearing small- to medium-sized buds. Nuclear inheritance also appears to be normal in *myo3Δ, myo5Δ*, mutants: fewer than 3% of cells examined display multinucleation (data not shown).

The myo3Δ,myo5Δ Mutant Displays Defects in Chitin Deposition and Cell Shape

Shortly before bud emergence, a ring of chitin is formed in the yeast cell wall. The bud then emerges within the confines of this chitin ring. After cell–cell separation, a chitin-containing ring is left on the surface of mother cells. Thus, chitin localization is an indicator of the polarity of bud site selection: haploid cells typically show an axial budding pattern and produce buds to previous bud sites. In contrast, diploid cells display a bipolar budding pattern and produce buds either adjacent to or at the pole opposite from previous bud sites (Roberts et al., 1983). Since polarization of actin cables and patches is disrupted in *myo3Δ,myo5Δ* double mutants, it was of interest to determine whether the polarized bud site selection and chitin deposition might also be affected.

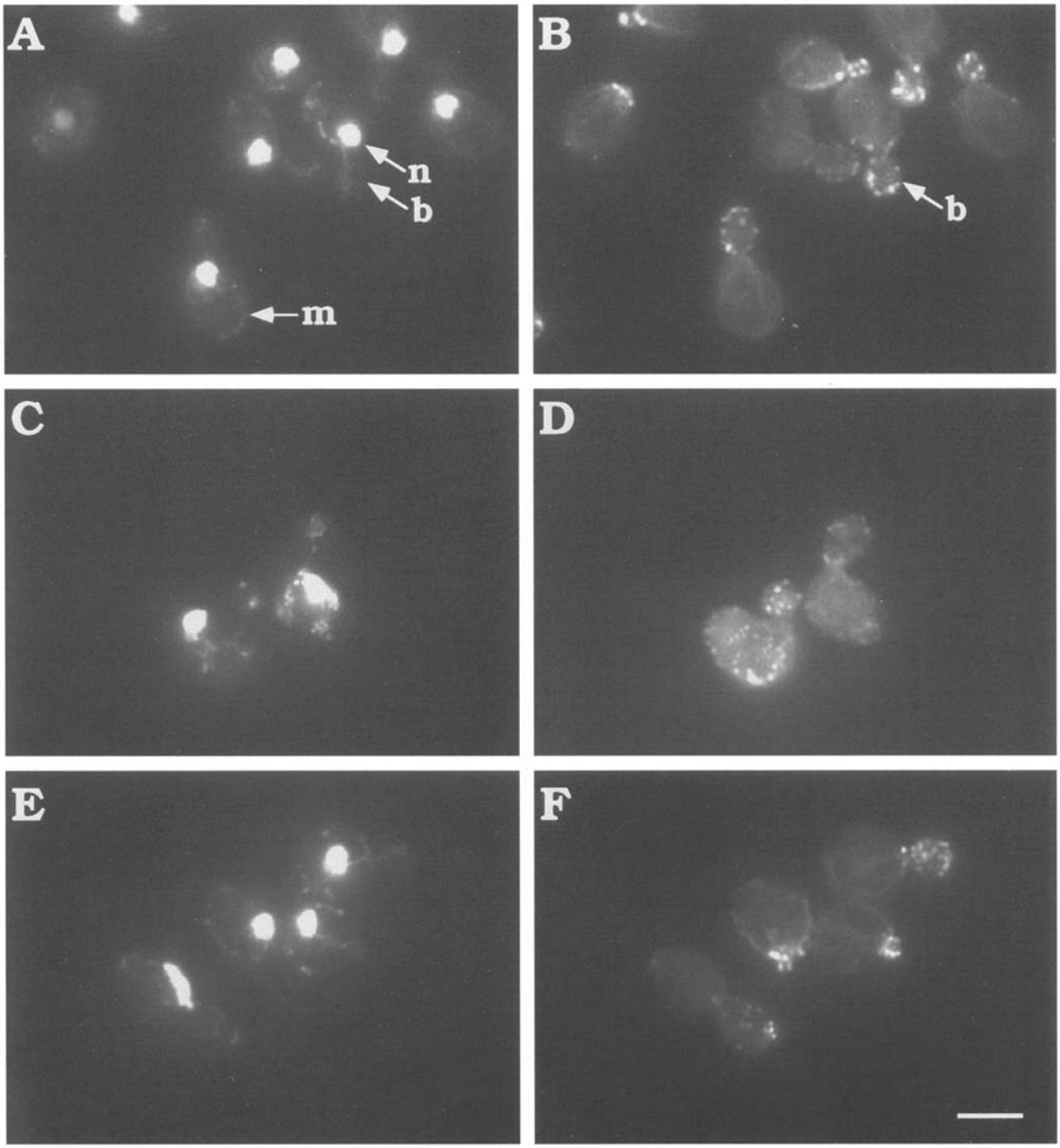

Figure 4. Actin, mitochondrial, and nuclear structure in wild-type cells, *myo3Δ,myo5Δ* double mutants and in double deletion mutants rescued with *MYO5* gene. Wild-type HA10-1b (*A* and *B*), *myo3Δ,myo5Δ* double deletion strain (HA31-9c; *C* and *D*), and *myo3Δ, myo5Δ* mutants rescued with *MYO5* on a low copy plasmid (*E* and *F*) were grown to mid-log phase at 30°C, fixed with paraformaldehyde, converted to spheroplasts, and stained with DAPI (*A*, *C*, and *E*) and rhodamine phalloidin (*B*, *D*, and *F*). DAPI staining reveals threads of mitochondria are inherited in all three strains (*A*, *C*, and *E*), but only the double mutant strain shows aggregation of mitochondria (*C*). Wild-type parental strain and *MYO5* rescued *myo3Δ,myo5Δ* double mutants show cortical actin patches polarized to the bud and actin cables prevalent in mother cells (*B* and *F*). Actin patches are randomly distributed over the surface of mother and bud in a large majority of *myo3Δ,myo5Δ* double mutant cells (*D*). *b*, bud; *m*, mitochondria; *n*, nucleus. Bar, 2 μm.

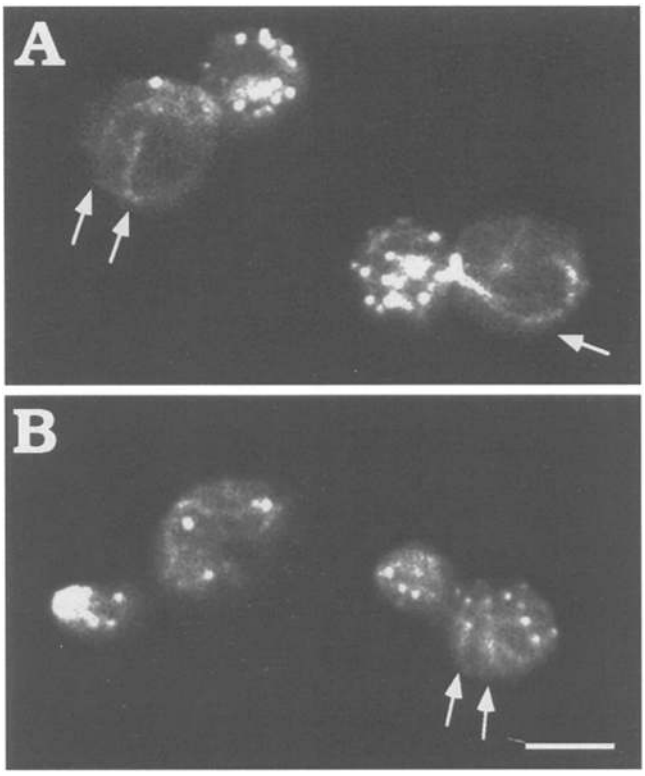

Figure 5. The *myo3Δ,myo5Δ* mutant displays defects in organization of yeast actin cables. Mid-log phase wild-type yeast (HA10-1b; *A*) and a *myo3Δ,myo5Δ* double mutant (HA31-9c; *B*) were stained with rhodamine-phalloidin as for Fig. 4. Actin cable structure was examined by confocal microscopy. The direction of the arrows illustrates the orientation of actin cables. Bar, 2 μm.

In wild-type cells, chitin rings are resolved as brightly stained rings using Calcofluor white (Fig. 6 *A*). These rings are normally restricted to one pole of the cell in haploid yeast. HA10-1b, a wild-type strain isogenic with myosin I single and double mutants, does not display the highly selective budding pattern expected of haploid yeast: bud site selection occurs both adjacent and distal to previous bud sites (Goodson and Spudich, 1995). The bud site selection pattern of haploid, myosin I single mutants is indistinguishable from that of HA10-1b (Fig. 6, *B* and *C*). 72% of cells have chitin rings that are restricted to the poles of the long axis of a mother cell.

The Calcofluor white staining pattern of the *myo3Δ, myo5Δ* double mutant is markedly different from that seen in wild-type or either single mutant (Fig. 6 *D*). Approximately 40% of budded cells display diffuse chitin deposition over the surface of the mother cell. Bright Calcofluor-stained patches, which are never detected in wild-type cells or in *myo3Δ* and *myo5Δ* single mutants, are present on 64% of double mutant cells. Chitin rings, which are distinct from chitin patches, are also detected in *myo3Δ, myo5Δ* mutants. However, only 23% of the double mutants contained chitin rings at polar regions of the cell. Thus, these mutants display defects in bud site selection during polarized cell growth and division. Finally, the diameter of bud scars is variable in *myo3Δ,myo5Δ* mutants with many of the scars being enlarged with respect to wild-type cells (data not shown).

Defects in size and shape of *myo3Δ,myo5Δ* mutants are also revealed by Calcofluor white stain. In wild-type yeast, early stages of bud growth are polarized and directed to the bud tip. Thereafter, growth is directed over the entire bud surface (Farkas et al., 1974). This pattern of bud growth produces oval shaped cells (Fig. 6 *A*). The length to width ratio of wild-type HA10-1b haploid yeast is 1.137 ± 0.109 (n = 179). Enlarged cells (>7 μm) are rare in wild-type cultures, accounting for <7% of the population during mid-log growth. Single mutations in either *MYO3* or *MYO5* lead to slightly rounder cells with a length to width ratio of 1.085 ± 0.087 (n = 144) and 1.065 ± 0.101 (n = 158), respectively, but there is no apparent accumulation of enlarged cells (Fig. 6, *B* and *C*). In contrast, >80% of double mutant cells are spherical or nearly spherical (Fig. 6 *D*), and a small but significant minority of cells (15%) are enlarged in comparison to wild-type cells (>7 μm in length).

Electron Microscopy Reveals Asymmetrically Thickened Cell Walls and Intracellular Membrane Accumulation in the myo3Δ,myo5Δ Mutant

The ultrastructure of *myo3Δ* mutant cells and *myo5Δ* mutant cells is similar to that of wild-type yeast cells (Fig. 7, *A–C*). A single large vacuole occupies a considerable portion of the cytoplasm, and a nucleus, mitochondria, and tubules of endoplasmic reticulum can be distinguished in most cells. When a mother–daughter pair is sectioned such that both cells and their bud neck are visible, all identifiable organelle structures are detected in transit through the bud neck into the daughter cell. Cell walls are resolved as an electron translucent inner portion 100–300-nm-thick surrounded by an electron dense shell of mannoproteins (reviewed in Klis, 1994).

The ultrastructure of vacuoles, mitochondria, ER, and nucleus is not significantly affected by deletion of *MYO3* and *MYO5*. However, 65% of budded *myo3Δ,myo5Δ* mutant cells accumulate multilamellar structures (Figs. 7 *D* and 8 *B*, *arrow*). These multilamellar organelles are ~200–500 nm in diameter and are often enriched in the bud. These structures resemble the "Berkeley Bodies" which have been previously described in late secretory mutants (Novick et al., 1981). Similar structures are not seen in wild-type cells or either single type I myosin mutant. Smaller vesicles (50–80-nm diam) also appear to accumulate in *myo3Δ,myo5Δ* mutants. These smaller vesicles are much less abundant than the multilamellar structures (Fig. 8 *B*, *arrowhead*).

myo3Δ,myo5Δ also display thickened cell walls. The cell walls of HA10-1b, the wild-type cell, and of *myo3Δ* and *myo5Δ* single mutant cells are 210 ± 38, 202 ± 34, and 212 ± 48 nm thick, respectively, and never exceeded a thickness of 500 nm. In contrast, 34% of *myo3Δ,myo5Δ* cells examined displayed cell walls which exceeded 500 nm; in some cells, wall thicknesses greater than 1 μm were observed. A pattern of concentric rings can be seen in many of the cells with extremely thick cell walls, suggesting that they are built through repeated deposition of cell wall material. In addition, virtually all cell wall thickening was detected in the mother cell: most buds display normal cell wall thickness.

To address whether defects in cell wall deposition and

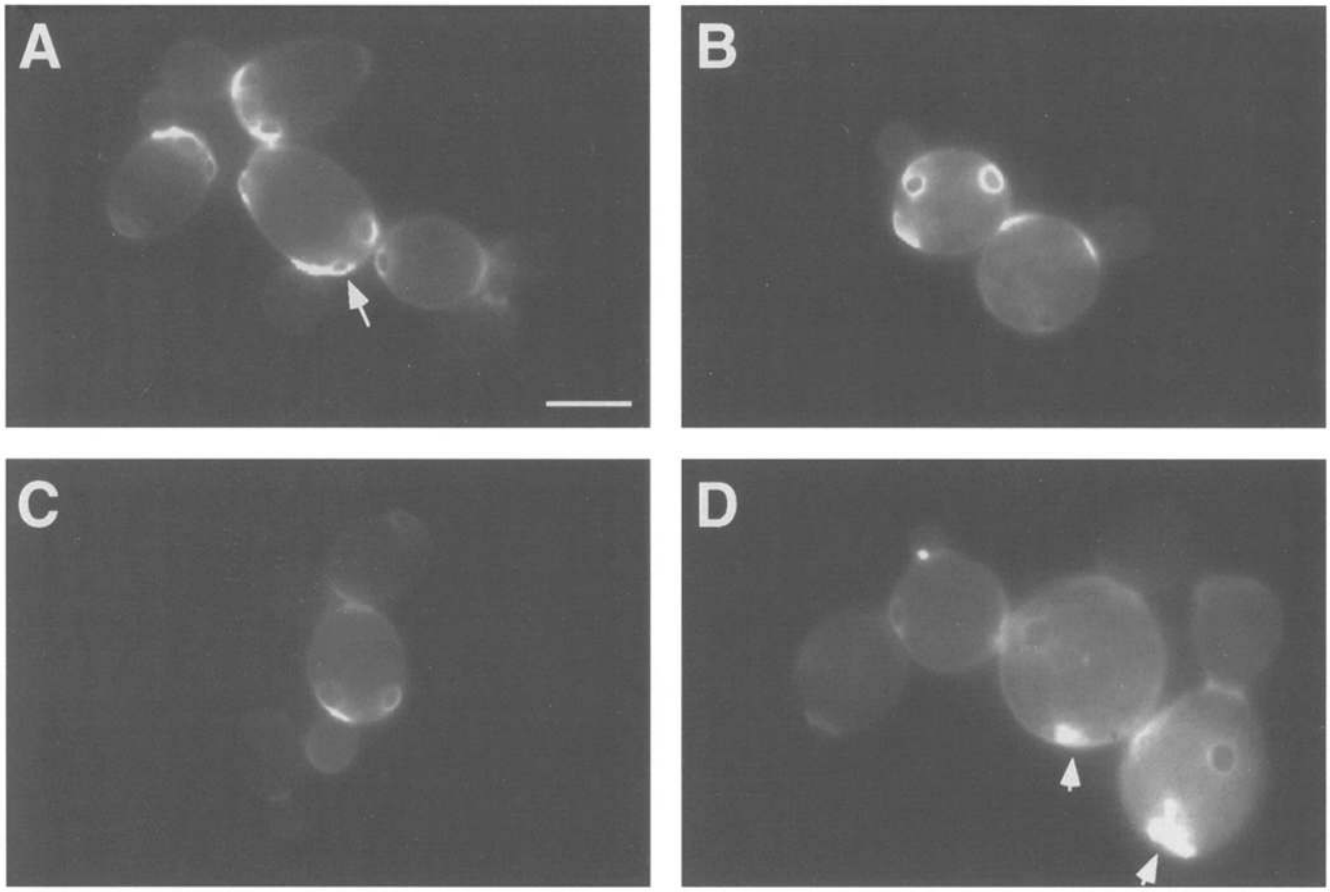

Figure 6. The *myo3Δ,myo5Δ* mutant displays defects in chitin deposition, cell size, and cell shape. Chitin in the cell walls of exponentially growing haploid wild-type (HA10-1b; *A*), *myo3Δ* mutant (HA31-9a; *B*), *myo5Δ* mutant (HA51-1a; *C*), and *myo3Δ,myo5Δ* mutant (HA31-9c; *D*) cultures was stained with Calcofluor white. Arrow (*A*) points to chitin rings which are localized at the poles of the mother cell in wild-type cells and single mutants, and randomly distributed in the *myo3Δ,myo5Δ* double mutant. Arrowheads (*D*) point to abnormal chitin patches detected in the *myo3Δ,myo5Δ* double mutant. Bar, 2 μm.

membrane accumulation observed in the *myo3Δ,myo5Δ* double mutant are consequences of long term perturbation of the actin cytoskeleton, we studied a mutant bearing defects in the actin-encoding *ACT1* gene. The temperature sensitive *act1-3* mutant used undergoes loss of actin cables at all conditions and temperature-dependent depolarization of actin patches (Novick and Botstein, 1985). At permissive temperature (22°C), *act1-3* cells display cell wall thickness similar to that of wild-type cells (Fig. 8 *C*). After short-term shift of the *act1-3* cells to 37°C, we observe modest cell wall thickening (Fig. 8 *D*). Moreover, we observe extensive cell wall thickening in *act1-3* mutants propagated at semi-permissive temperatures (30°C) for multiple generations (data not shown). These observations are consistent with a previous report that cell wall thickening occurs in actin mutants incubated at restrictive temperatures for prolonged time periods (Gabriel and Kopecká, 1995).

The actin mutant also displays abnormal intracellular membrane accumulation. At 22°C, *act1-3* cells display some small vesicle accumulation (Fig. 8 *C*). After shift to restrictive temperature (37°C) for 45 min, these mutants show accumulation of both small vesicles and multilamellar vesicles (Fig. 8 *D*). The levels of accumulated membranes differ in the actin mutant compared to the myosin I double deletion mutant. In the *myo3Δ,myo5Δ* double mutant multilamellar structures are abundant and small vesicles are rare. In contrast, small vesicles are abundant and multilamellar structures are rare in *act1-3* cells after short term shift to 37°C. However, upon propagation of the actin mutant at a semi-restrictive temperature (30°C), the amount of multilamellar structures and 50–80 nm vesicles in the *act1-3* strain is similar to that in the myosin I double deletion mutant (data not shown). These findings suggest that defects in cell wall deposition and membrane accumulation observed in the *myo3Δ,myo5Δ* double mutant are consequences of long-term perturbation of actin cytoskeletal organization.

myo3Δ,myo5Δ Mutants Display Defects in Invertase Secretion and Fluid Phase Endocytosis

Accumulation of intracellular membranes in the *myo3Δ, myo5Δ* double mutants suggests possible defects in membrane trafficking. Therefore, we examined the effect of myosin I gene deletion on invertase secretion and fluid phase endocytosis of Lucifer yellow. Invertase is a highly glycoslyated, secretory protein which catalyzes cleavage of α-glycosidic

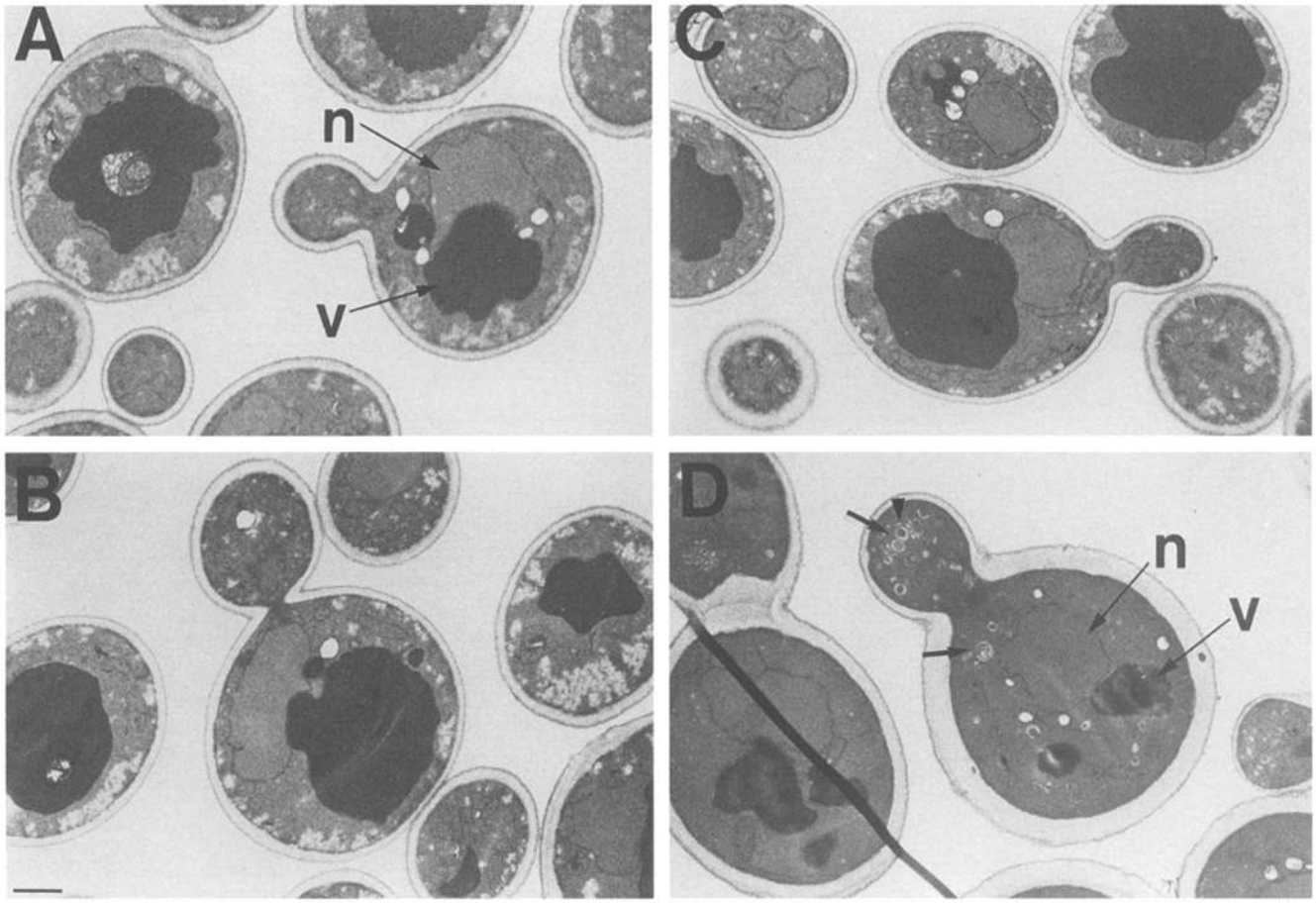

Figure 7. The *myo3Δ,myo5Δ* mutant displays cell wall thickening and intracellular accumulation of membranes. Wild-type (HA10-1b; *A*), *myo3Δ* mutant (HA31-9a; *B*), *myo5Δ* mutant (HA51-1a; *C*), and *myo3Δ,myo5Δ* mutant (HA31-9c; *D*) cells were grown to mid-log phase at 30°C. Cells were fixed with glutaraldehyde, stained with $KMnO_4$, embedded, and sectioned. Arrows indicate large multilamellar vesicles; Arrowheads indicate small vesicles; *n*, nucleus; *v*, vacuole. Bar, 1 μm.

linkages and is required for growth using many di- and trisaccharides as a carbon source. The *myo3Δ,myo5Δ* double mutant displays low but detectable growth on medium containing the trisaccharide raffinose. While poor growth on raffinose is consistent with a defect in invertase secretion, this result is difficult to interpret because the double mutant also displays poor growth on galactose and glycerol (data not shown). However, defects in the rate of invertase secretion can also be shown biochemically (Fig. 9). Wild-type cells secrete invertase immediately after induction of invertase expression and display a maximal level of external invertase within 90 min. In contrast, *myo3Δ,myo5Δ* mutants display a delay in the onset of invertase secretion after induction. Analysis of intracellular invertase revealed accumulation of partially processed glycosylation intermediates during this initial lag phase (data not shown). Thus, the double mutant is capable of responding to induction, but displays defects in the invertase secretion pathway. Invertase secretion is detected within 60 min after induction of the myosin I double mutant and occurs at rates similar to that of isogenic wild-type strains up to 180 min after induction. The maximum level of invertase secretion in the mutant is 25% greater than that of the wild-type cell. It is possible that the thickened cell wall of the myosin double deletion mutant retains greater levels of secreted invertase.

Lucifer yellow is a hydrophilic fluorescent dye which is excluded from cells by their plasma membrane. Yeast take up Lucifer yellow by fluid phase endocytosis and target the dye to their vacuole (Riezman, 1985). Mutations affecting actin or the actin binding protein Sac6p perturb this process (Kübler and Riezman, 1993). Lucifer yellow uptake into the vacuole is observed in >90% of wild-type HA10-1b cells after 30 min of incubation. In contrast, Lucifer yellow uptake and accumulation in the vacuole was observed in only 10% of *myo3Δ,myo5Δ* mutants under the same experimental conditions (Fig. 10). After 120 min of incubation with Lucifer yellow, the percentage of double mutant cells with labeled vacuoles was unchanged. Thus, deletion of myosin I genes compromises fluid phase endocytosis in yeast.

Myo5p Co-localizes with Actin Patches

To determine the subcellular localization of Myo5p, the wild-type *MYO5* gene was tagged with three copies of the myc epitope, and expressed in the *myo3Δ,myo5Δ* mutant. To insure that myc-tagged Myo5p was expressed at levels

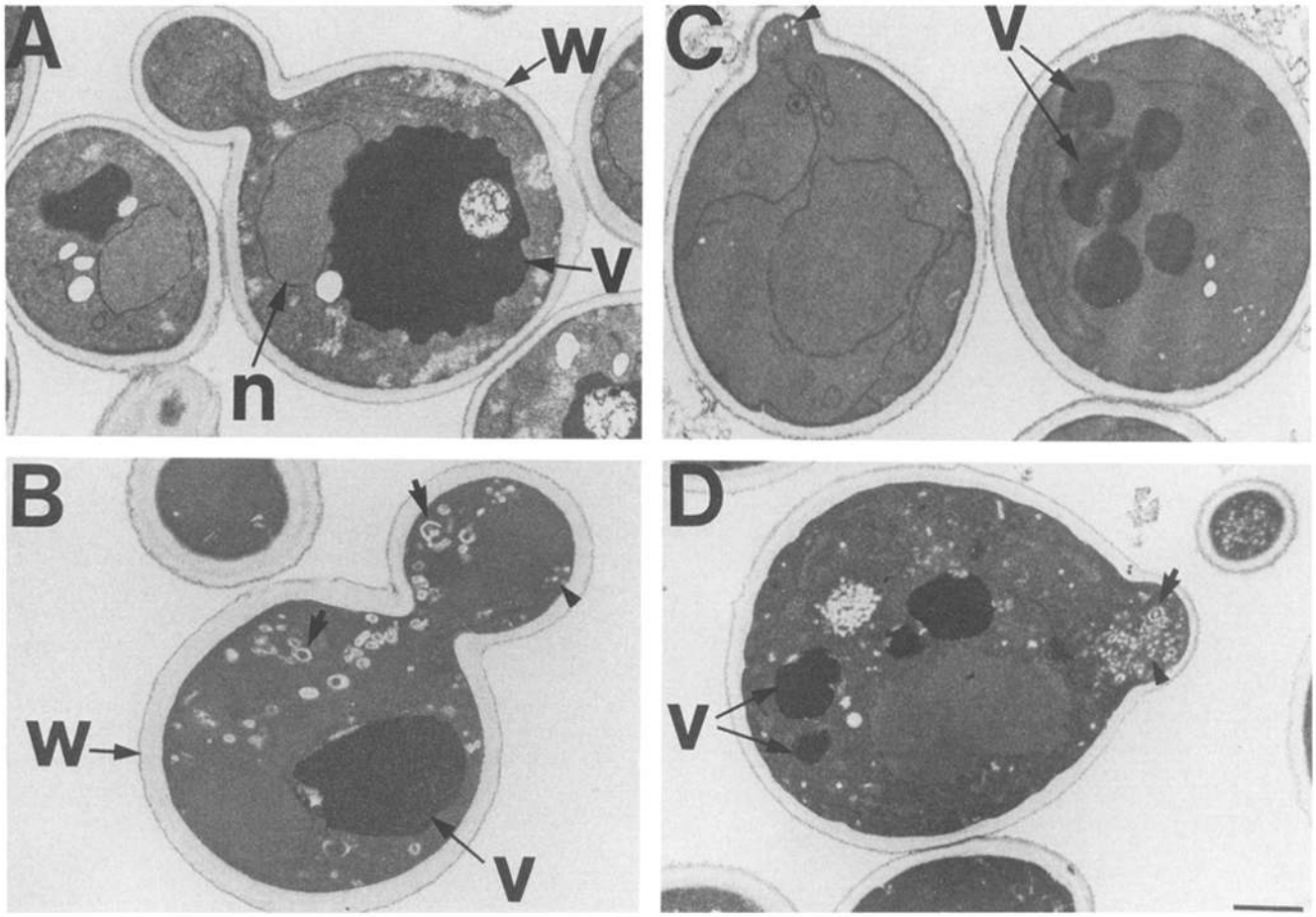

Figure 8. Cell wall thickening and accumulation of vesicles and multilamellar membranes occur in *act1-3* mutants. Wild-type cells (HA10-1b) and *myo3Δ,myo5Δ* double mutants (HA31-9c) were prepared for electron microscopy as for Fig. 7. Temperature sensitive *act1-3* mutants were grown at permissive temperature (22°C) to mid-log phase. An aliquot of this culture was incubated at restrictive temperature (37°C) for 45 min, and cultures were fixed and prepared for electron microscopy as for Fig. 7. Representative images of HA10-1b wild-type (*A*), *myo3Δ,myo5Δ* double mutant (*B*), *act1-3* conditional mutant at a growth permissive temperature (*C*), and *act1-3* mutant after short term shift to restrictive temperature (*D*) are shown. Arrows indicate large multilamellar vesicles. Arrowheads indicate small vesicles. *n*, nucleus; *v*, vacuole; *w*, cell wall. Bar, 1 μm.

similar to that of wild-type Myo5p, expression was carried out using a low copy, centromere-based plasmid under control of the endogenous *MYO5* upstream sequences. As described above, expression of the epitope-tagged Myo5p in the *myo3Δ,myo5Δ* mutant restores normal growth rates (Table II). Therefore, addition of the myc tag to the COOH terminus of Myo5p does not appear to have a deleterious effect on Myo5p function.

The expression and detection of the tagged protein was evaluated using Western blot analysis (Fig. 11 *a*) and indirect immunofluorescence (Fig. 11 *b*). We find that the anti-myc monoclonal antibody 9E10 (Evan et al., 1985) recognizes a single band in whole cell extracts of myc-Myo5p–expressing cells (Fig. 11 *A*). The antibody does not recognize any protein in the *myo3Δ,myo5Δ* mutant or in a *myo3Δ,myo5Δ* mutant expressing untagged Myo5p. The electrophoretic mobility of the band detected in myc-Myo5p–expressing cells, 135 kD, is in good agreement with the size predicted from the DNA sequence of the *MYO5* gene. Double label indirect immunofluorescence experiments indicate that myc-tagged Myo5p localizes with actin patches (Fig. 11 *B*). Within the bud, myc-tagged Myo5p is detected in some, but not all, of the actin patches. In addition, we observe co-localization of myc-tagged Myo5p with actin patches that accumulate at the site of bud emergence. myc-tagged Myo5p was not detected in actin cables.

Discussion

Myosin I's are ubiquitous proteins expected to play an important role in cytoskeletal function. In a previous study, the first yeast myosin I was identified (Goodson and Spudich, 1995). This classic myosin I protein is encoded by the *MYO3* gene. Deletion of this gene has no obvious effect. This raised the possibility that yeast contain other protein(s) with redundant function(s). Our approach to study myosin I function was to use a synthetic lethality screen to identify yeast proteins which are functionally redundant with Myo3p. This screen revealed a new classic myosin I gene, *MYO5*. *MYO5* is 75.4% identical to *MYO3*. Both genes contain coding regions for motor and tail sub-domains typical of a classic myosin I including a basic (possible membrane-binding) region, an SH3 domain, and a proline-rich

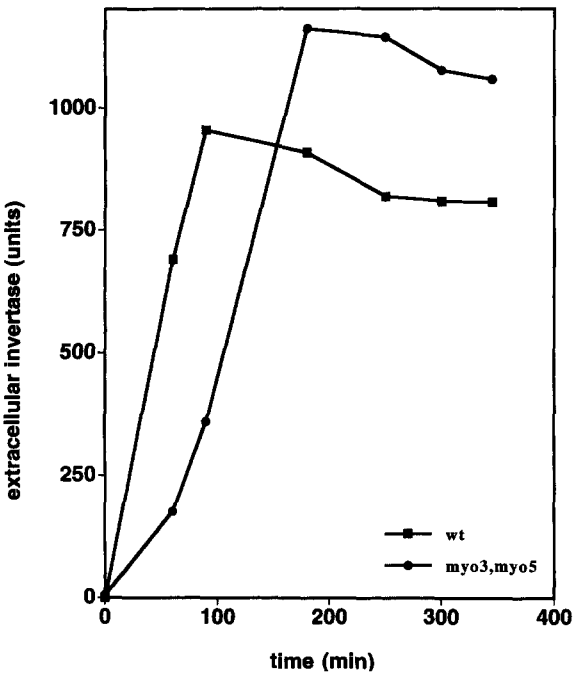

Figure 9. Invertase secretion is defective in mutants bearing deletions of *MYO3* and *MYO5*. Wild-type (HA10-1b) and *myo3Δ, myo5Δ* mutant (HA31-9c) cells were grown to mid-log phase at 30°C and transferred to growth media containing 0.05% glucose to derepress the expression of invertase. Aliquots were taken at the indicated times and assayed for external invertase.

region (for review see Hammer, 1991). Deletion of either *MYO3* or *MYO5* has no obvious phenotype. However, we show that a yeast strain bearing deletions of both *MYO3* and *MYO5* displays severe growth defects, enlarged cell size, delocalized and disorganized chitin deposition, asymmetrically thickened cell walls, disruption in the normal polar distribution of actin, accumulation of abnormal membrane bound structures and growth defects under conditions of osmotic stress, low pH , low temperature and elevated temperature. Our findings indicate that yeast *MYO3* and *MYO5* genes encode classic myosin I proteins with overlapping function. These results are the first genetic demonstration that myosin I proteins are required for normal cell function in yeast.

The phenotype of the myosin I double deletion mutant is similar to that of yeast strains bearing mutations that perturb the actin cytoskeleton. For example, mutation of actin (*ACT1*) or the actin-binding proteins fimbrin (*SAC6*), capping protein (*CAP1-2*), profilin (*PFY1*), or myosin V (*MYO2*) leads to most or all of the following phenotypes: partial or complete loss of actin cables, actin patch depolarization, rounded cell shape, random bud site selection, vesicle and membrane accumulation, cell wall thickening, sensitivity to high osmotic strength, defects in chitin deposition, invertase secretion, endocytosis, and mitochondrial organization (Novick and Botstein, 1985; Haarer et al., 1990; Rodriguez and Patterson 1990; Adams et al., 1991; Johnston et al., 1991; Amatruda et al., 1992; Chowdhury et al., 1992; Liu and Bretscher, 1992; Kübler and Riezman, 1993; Drubin et al., 1993; Lazzarino et al., 1994; Simon et al., 1995). One distinguishing feature of the myosin I double deletion mutant is that the depolarization of actin structures occurs without a significant reduction in the amount of either actin cables or patches. This, coupled with the observation that the phenotype of the myosin I double deletion mutant is similar to that of strains with mutations in actin or actin-binding proteins, supports a role for Myo3p and Myo5p in control of actin cable and patch polarization. At present, this myosin I double deletion mutant and cells bearing mutations in the *SLA1*, *RVS161*, or *RVS167* genes are the only yeast mutants defective specifically in actin organization (Bauer et al., 1993; Holtzman et al., 1993; and Silvadon et al., 1995). However, since actin cables are difficult to detect in *myo3Δ,myo5Δ* mutants by epifluorescence microscopy, it is possible that other mutants thought to have a significant reduction in actin cables may instead have a similar loss of actin organization.

Since myosin I proteins have been implicated in control of membrane–actin interactions, it is possible that Myo3p and Myo5p serve as organelle motors for vesicle movement during endocytosis and secretion. This interpretation is consistent with the postulated function of classic myosin I proteins in *Aspergillus* (McGoldrick et al., 1995). However, actin organization is altered upon deletion of yeast myosin I genes. In addition, actin is known to be necessary for secretion and endocytosis in yeast. Therefore, we favor the interpretation that the primary function of yeast myosin I proteins is control of actin organization, and we propose that the observed defects in secretion, endocytosis, and osmotic sensitivity are secondary effects due to loss of actin organization.

This interpretation is supported by the finding that Myo5p is present in actin patches. Indirect immunofluorescence and epitope-tagging were used to determine the localization of Myo5p. We find that the myc-tagged protein is fully functional and observe co-localization of myc-tagged Myo5p with actin patches under conditions where the tagged protein was expressed at levels similar to wild-type Myo5p. Previous studies suggest that (*a*) actin patches are invaginations in the plasma membrane that are associated with F-actin (Mullholland et al., 1994), and (*b*) actin nucleation and assembly occur at actin patches in the bud of small-budded cells. This nucleation activity requires the *SLA1* and *SLA2* gene products and may be regulated by Cdc42p, a Rho-like GTP binding protein (Li et al., 1995). Thus, the finding that Myo5p is localized at actin patches is consistent with a model whereby myosin I proteins are required for polarization of the actin cytoskeleton. In princi-

Figure 11. Localization of myc-tagged Myo5p at actin patches. (*a*) Whole cell extracts from the *myo3Δ,myo5Δ* mutant (lane *1*), *myo3Δ,myo5Δ* mutant expressing untagged *MYO5* (lane *2*), and *myo3Δ,myo5Δ* mutant expressing myc-tagged *MYO5* (lane *3*) were analyzed by Western blot analysis using a monoclonal anti-myc antibody. The antibody recognizes a band with the predicted molecular weight of myc-tagged Myo5p only in cells expressing epitope-tagged *MYO5*. (*b*) Mid-log phase *myo3Δ,myo5Δ* mutants transformed with plasmid bearing *MYO5* (*A* and *C*) or myc-tagged *MYO5* (*B* and *D*) were fixed and converted to spheroplasts, as described above.

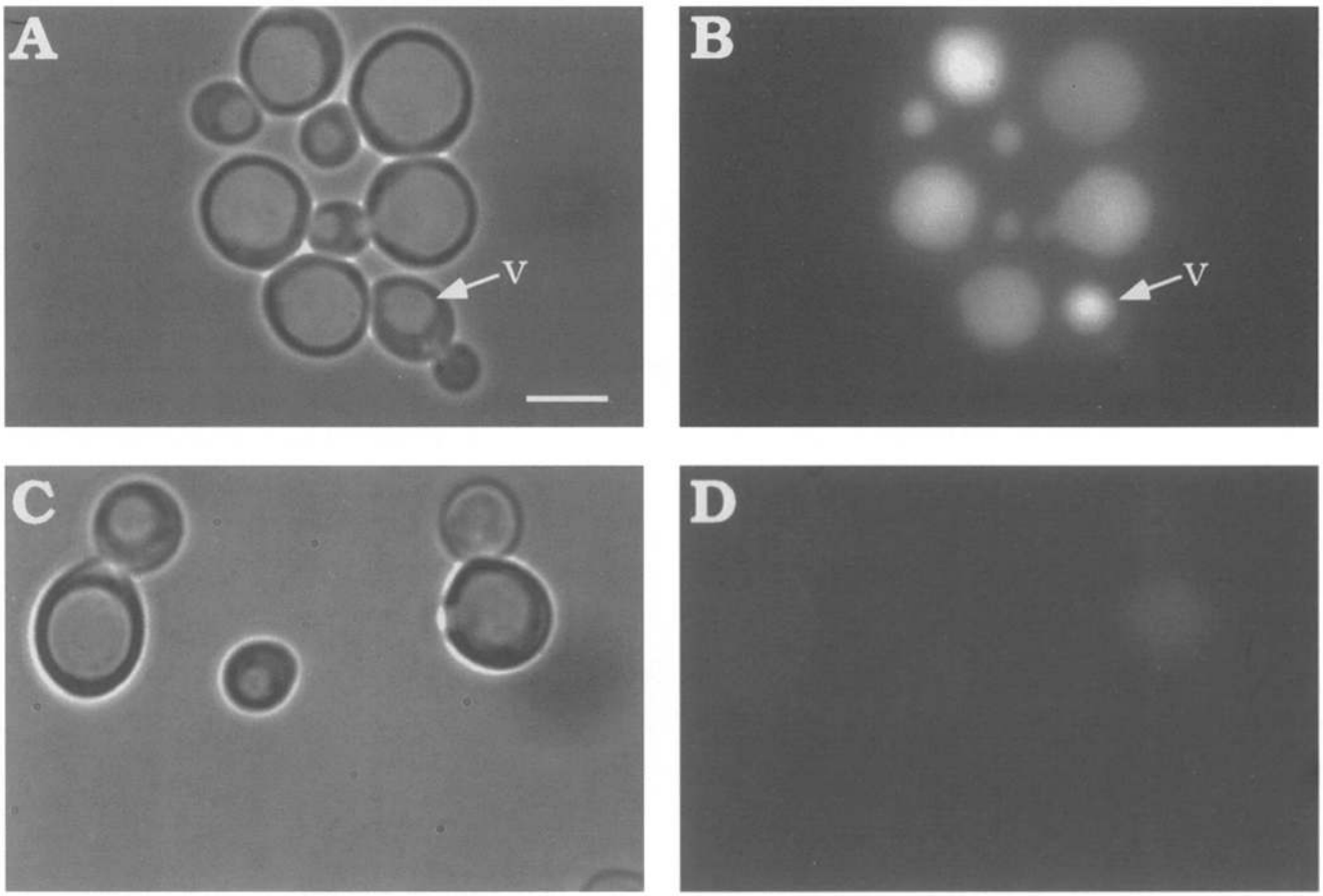

Figure 10. Uptake of Lucifer yellow is defective in the *myo3Δ,myo5Δ* mutants. Mid-log phase wild-type (HA10-1b; *A* and *B*) and *myo3Δ,myo5Δ* mutant (HA31-9c; *C* and *D*) cultures were incubated with Lucifer yellow (4 mg/ml) for 120 min at 30°C. (*A* and *C*) phase contrast images; (*B* and *D*) fluorescence images showing Lucifer yellow uptake into the vacuole; *v*, vacuole. Bar, 2 μm.

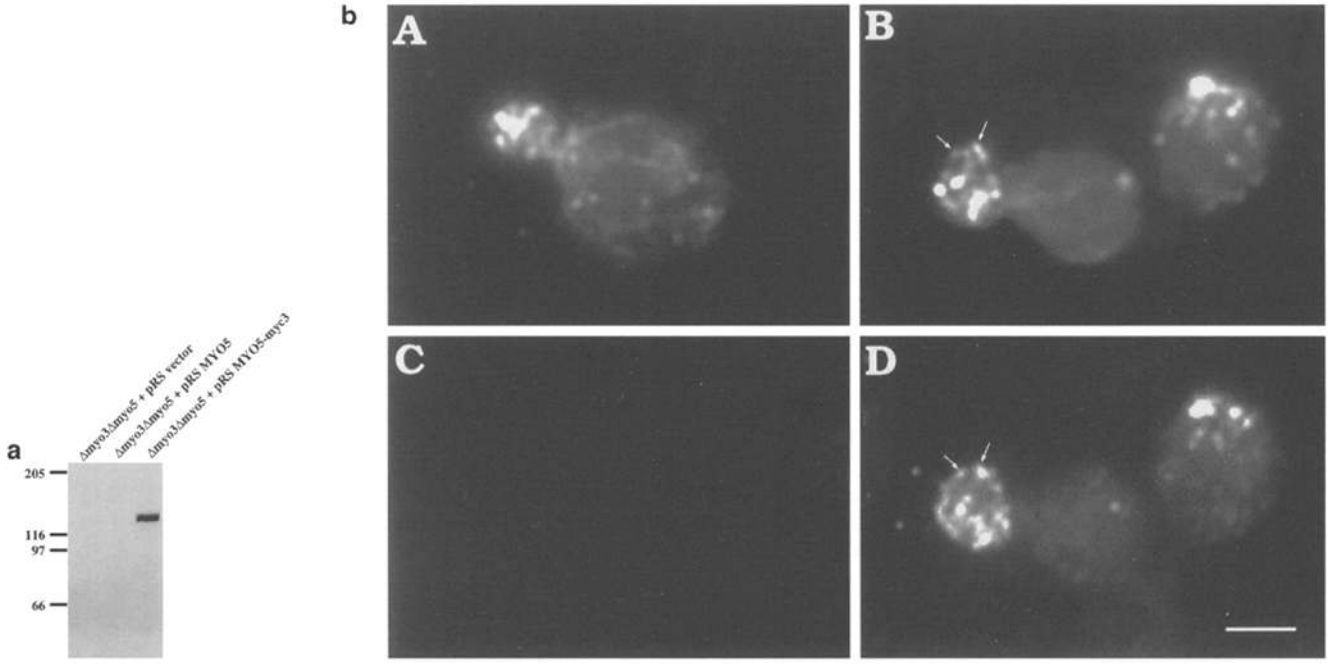

In this double label experiment, actin (*A* and *B*) and myc-tagged Myo5p (*C* and *D*) were visualized using a polyclonal antibody raised against yeast actin and a mouse anti-myc monoclonal antibody. Arrows indicate cortical actin patches which co-localize with myc-tagged Myo5p. Bar, 1 μm.

ple, targeting of myosin I proteins to membrane–cytoskeletal junctions may be controlled by SH3 and possible membrane binding subdomains found in the tail domain. In addition, translocation of F-actin along microfilament tracks, and/or ATP-sensitive actin cross-linking during actin reorganization and polarization may be mediated by the ATP-insensitive and sensitive actin binding sites in the tail and motor domains.

Although *myo3Δ,myo5Δ* double mutants share phenotypes with other mutants which perturb actin structure, the severity of specific phenotypes differs among mutants. For example, the temperature-sensitive *act1-3* mutant displays severe defects in mitochondrial organization and motility, accumulation of high levels of 50-nm vesicles, and only limited accumulation of multilamellar structures which resemble Berkeley bodies (Novick and Botstein, 1985; Drubin et al., 1993; Lazzarino et al., 1994; Simon et al., 1995). In contrast, deletion of both yeast myosin I genes results in accumulation of high levels of multilamellar structures and only minor defects in mitochondrial organization and 50-nm vesicle accumulation. We observe that some of these differences are due to chronic versus acute actin disorganization. However, it is also possible that the variation in phenotype severity reflects differential dependence of different processes on actin cables and actin patches. As described above, deletion of *MYO3* and *MYO5* results in defects in polarization of actin cable and patch structures without significantly affecting the number of actin patches and cables. In contrast, *act1-3* mutants show complete loss of actin cables under all conditions and depolarized actin patches only at restrictive temperature. Therefore, it is possible that mitochondria, which co-localize with actin cables (Drubin et al., 1993; Lazzarino et al., 1994), may be more severely compromised in mutants like *act1-3* which do not contain these actin structures. In contrast, the relatively strong effect of the deletion of *MYO3* and *MYO5* on endocytosis may reflect a dependence of this process on the specific organization of cytoskeletal elements, possibly at a very local level.

The conservation of classic myosin I proteins in evolutionarily divergent organisms (Goodson and Spudich, 1993; Cheney et al., 1993) suggests that they have a significant role in many eukaryotic cell types. It has long been postulated that myosin I proteins play a role in the generation of cell motility (for review, see Pollard et al., 1991; Spudich and Warrick, 1991). Results from analysis of *Dictyostelium* myosin I mutants support this idea (Titus et al., 1993). Here, we show that two classic myosin I proteins are important for cell growth in an organism which does not move. Similar results were obtained recently in *Aspergillus* (McGoldrick et al., 1995). These results demonstrate that classic myosin I proteins are fundamentally important to the function of non-motile cells and suggest that they have a key role in cytoskeletal processes common to both motile and non-motile cells. More specifically, we provide evidence that (*a*) *MYO3* and *MYO5* encode myosin I proteins with overlapping function, and (*b*) these classic myosin I proteins are necessary for control of actin polarity in yeast. Our results in yeast, together with recent results in *Dictyostelium* (Novak et al., 1995), suggest that myosin I proteins play an important organizational role in the actin cytoskeleton in many eukaryotes.

We thank Dr. L.A. Greene for support and encouragement; H. O'Sullivan for expert assistance with the electron microscopy; M. Smith for assistance in use of the confocal microscope; Dr. D.G. Drubin for anti-actin antibody; Dr. D. Eshel for the plasmid bearing the myc epitope; and B. Patterson, K. Redding, and J. McCusker for invaluable discussions and advice in the yeast manipulations.

This work was supported by National Institutes of Health grants GM40509 to James A. Spudich and GM45735 to Liza A. Pon, and a Medical Scientists Training Program Award, 5T32 GM07367, to Blake L. Anderson.

Received for publication 18 January 1996 and in revised form 4 April 1996.

References

Adams, A.E., D. Botstein, and D.G. Drubin. 1991. Requirement of yeast fimbrin for actin organization and morphogenesis *in vivo*. *Nature (Lond.)*. 354: 404–408.

Adams, R.J., and T.D. Pollard. 1989. Binding of myosin I to membrane lipid. *Nature (Lond.)*. 340:565–568.

Amatruda, J.F., D.J. Gattermeir, T.S. Karpova, and J.A. Cooper. 1992. Effects of null mutations and overexpression of capping protein on morphogenesis, actin distribution and polarized secretion in yeast. *J. Cell Biol.* 119:1151–1162.

Bauer, F., M. Urdaci, M. Aigle, and M. Crouzet. 1993. Alteration in a yeast SH3 protein leads to conditional viability with defects in cytoskeletal and budding patterns. *Mol. Cell. Biol.* 13:5070–5084.

Bender, A., and J.R. Pringle. 1991. Use of a screen for synthetic-lethal and multicopy-suppressee mutants to identify two new genes involved in morphogenesis in *Saccharomyces cerevisiae*. *Mol. Cell. Biol.* 11:1295–1305.

Cheney, R.E., and M.S. Mooseker. 1992. Unconventional myosins. *Curr. Biol.* 4:27–35.

Cheney, R.E., M.A. Riley, and M.S. Mooseker. 1993. Phylogenetic analysis of the myosin superfamily. *Cell Motil. Cytoskeleton.* 24:215–223.

Chowdhury, S., K.W. Smith, and M.C. Gustin. 1992. Osmotic stress and the actin cytoskeleton: phenotype-specific suppression of an actin mutation. *J. Cell Biol.* 118:561–571.

Christianson, T.W., R.S. Sikorski, M. Dante, J.H. Shero, and P. Hieter. 1992. Multifunctional yeast high-copy-number shuttle vectors. *Gene.* 110:119–122.

Doberstein, S.K., and T.D. Pollard. 1992. Localization and specificity of the phospholipid and actin binding sites on the tail of *Acanthamoeba* myosin IC. *J. Cell Biol.* 117:1241–1249.

Doberstein, S.K., I.C. Baines, G. Wiegand, E.D. Korn, and T.D. Pollard. 1993. Inhibition of contractile vacuole function *in vivo* by antibodies against myosin-1. *Nature (Lond.)*. 365:841–843.

Drubin, D.G., H.D. Jones, and K.F. Wertman. 1993. Actin structure and function: roles in mitochondrial organization and morphogenesis in budding yeast and identification of the phalloidin-binding site. *Mol. Biol. Cell.* 4: 1277–1294.

Drubin, D.G., K.G. Miller, and D. Botstein. 1988. Yeast actin-binding proteins: evidence for a role in morphogenesis. *J. Cell Biol.* 107:2551–2561.

Evan, G.I., G.K. Lewsi, G. Ramsay, and J.M. Bishop. 1985. Isolation of monoclonal antibodies specific for human c-myc proto-oncogene product. *Mol. Cell. Biol.* 5:3610–3616.

Falco, S.C., and K.S. Dumas. 1985. Genetic analysis of mutants of *Saccharomyces cerevisiae* resistant to the herbicide sulfometuron methyl. *Genetics.* 109: 21–35.

Falco, S.C., K.S. Dumas, and K.J. Livak. 1985. Nucleotide sequence of the yeast *ILV2* gene which encodes acetolactate synthase. *Nucleic Acids Res.* 13:4011–4027.

Farkas, V., J. Kovarik, A. Kosinova, and S. Bauer. 1974. Autoradiographic study of mannan incorporation into the growing walls of *Saccharomyces cerevisiae*. *J. Bacteriol.* 117:265–269.

Gabriel, M., and M. Kopecká. 1995. Disruption of the actin cytoskeleton in budding yeast results in formation of an aberrant cell wall. *Microbiol.* 141: 891–899.

Goldstein, A., and J.O. Lampen. 1975. Beta-D-fructofuranoside fructohydrolase from yeast. *Methods Enzymol.* 42:504–511.

Goodson, H.V., and J.A. Spudich. 1993. Molecular evolution of the myosin family: relationships derived from comparisons of amino acid sequences. *Proc. Natl. Acad. Sci. USA.* 90:659–663.

Goodson, H.V., and J.A. Spudich. 1995. Identification and molecular characterization of a yeast myosin I. *Cell Motil. Cytoskeleton.* 30:73–84.

Guthrie, C., and G.R. Fink. 1991. Guide to Yeast Genetics and Molecular Biology. *Methods in Enzymology.* Vol. 194. Academic Press, Inc., San Diego, CA.

Haarer, B.K., S.H. Lillie, A.E. Adams, V. Magdolen, W. Bandlow, and S.S. Brown. 1990. Purification of profilin from *Saccharomyces cerevisiae* and analysis of profilin-deficient cells. *J. Cell Biol.* 110:105–114.

Haarer, B.K., A. Petzold, S.H. Lillie, and S.S. Brown. 1994. Identification of MYO4, a second class V myosin gene in yeast. *J. Cell. Sci.* 107:1055–1064.

Hammer, J.A. 1991. Novel myosins. *Trends Cell Biol.* 1:50–56.

Hammer, J.A., G. Jung, and E.D. Korn. 1986. Genetic evidence that *Acanthamoeba* myosin I is a true myosin. *Proc. Natl. Acad. Sci. USA.* 83:4655–4659.

Hasson, T., and M.S. Mooseker. 1995. Molecular motors, membrane movement and physiology: emerging roles for myosins. *Curr. Opin. Cell Biol.* 7:587–594.

Holtzman, D.A., S. Yang, and D.G. Drubin. 1993. Synthetic-lethal interactions identify two novel genes, SLA1 and SLA2, that control membrane cytoskeleton assembly in *Saccharomyces cerevisiae. J. Cell Biol.* 122:635–644.

Huffaker, T.C., M.A. Hoyt, and D. Botstein. 1987. Genetic analysis of the yeast cytoskeleton. *Annu. Rev. Genet.* 21:259–284.

Johnston, G.C., J.A. Prendergast, and R.A. Singer. 1991. The *Saccharomyces cerevisiae MYO2* gene encodes an essential myosin for vectorial transport of vesicles. *J. Cell Biol.* 113:539–551.

Jung, G., and J.A. Hammer. 1990. Generation and characterization of *Dictyostelium* cells deficient in a myosin I heavy chain isoform. *J. Cell Biol.* 110(6): 1955–1964.

Jung, G., and J.A. Hammer. 1994. The actin binding site in the tail domain of *Dictyostelium* myosin IC (myoC) resides within the glycine- and proline-rich sequence (tail homology region 2). *FEBS Lett.* 342:197–202.

Jung, G., Y. Fukui, B. Martin, and J.A. Hammer. 1993. Sequence, expression pattern, intracellular localization, and targeted disruption of the *Dictyostelium* myosin ID heavy chain isoform. *J. Biol. Chem.* 268:14981–14990.

Klis, F.M. 1994. Review: Cell wall assembly in yeast. *Yeast.* 10:851–869.

Kübler, E., and H. Riezman. 1993. Actin and fimbrin are required for the internalization step of endocytosis in yeast. *EMBO (Eur. Mol. Biol. Org.) J.* 12: 2855–2862.

Lawrence, C.W. 1991. Classical mutagenesis techniques. *Methods Enzymol.* 194:273–281.

Lazzarino, D., I. Boldogh, M.G. Smith, J. Rosand, and L.A. Pon. 1994. Yeast mitochondria contain ATP-sensitive, reversible actin-binding activity. *Mol. Biol. Cell.* 5:807–818.

Li, R., Y. Aheng, and D.G. Drubin. 1995. Regulation of cortical actin cytoskeleton assembly during polarized cell growth in budding yeast. *J. Cell Biol.* 128:599–615.

Liu, H., and A. Bretscher. 1992. Characterization of *TPM1* disrupted yeast cells indicates an involvement of tropomyosin in directed vesicular transport. *J. Cell Biol.* 118:285–299.

Lynch, T.J., J.P. Albanesi, E.D. Korn, E.A. Robinson, B. Bowers, and H. Fujisaki. 1986. ATPase activities and actin-binding properties of subfragments of *Acanthamoeba* myosin IA. *J. Biol. Chem.* 261:17156–17162.

McGoldrick, C.A., C. Gruver, and G.S. May. 1995. MyoA of *Aspergillus nidulans* encodes an essential myosin I required for secretion and polarized growth. *J. Cell Biol.* 128:577–587.

Mulholland, J., D. Preuss, A. Moon, A. Wong, D. Drubin, and D. Botstein. 1994. Ultrastructure of the yeast actin cytoskeleton and its association with the plasma membrane. *J. Cell Biol.* 125:381–391.

Novak, K.D., M.D. Peterson, M.C. Reedy, and M.A. Titus. 1995. *Dictyostelium* myosin I double mutants exhibit conditional defects in pinocytosis. *J. Cell Biol.* 131:1205–1221.

Novick, P., and D. Botstein. 1985. Phenotypic analysis of temperature sensitive yeast actin mutants. *Cell.* 40:405–416.

Novick, P., S. Ferro, and R. Schekman. 1981. Order of events in the yeast secretory pathway. *Cell.* 25:461–469.

Pollard, T.D., and E.D. Korn. 1973. *Acanthamoeba* myosin. I. Isolation from *Acanthamoeba castellanii* of an enzyme similar to muscle myosin. *J. Biol. Chem.* 248:4682–4690.

Pollard, T.P., S.K. Doberstein, and H.G. Zot. 1991. Myosin-I. *Annu. Rev. Physiol.* 53:653–681.

Pringle, J.R., A.E. Adams, D.G. Drubin, and B.K. Haarer. 1991. Immunofluorescence methods for yeast. *Methods Enzymol.* 194:565–601.

Riezman, H. 1985. Endocytosis in yeast: several of the yeast secretory mutants are defective in endocytosis. *Cell.* 40:1001–1009.

Roberts, R.L., N. Bowers, M.L. Slater, and E. Cabib. 1983. Chitin synthesis and localization in cell division cycle mutants of *Saccharomyces cerevisiae. Mol. Cell Biol.* 3:922–930.

Rodriguez, J.R., and B.M. Paterson. 1990. Yeast myosin heavy chain mutant: maintenance of the cell type specific budding pattern and the normal deposition of chitin and cell wall components requires an intact myosin heavy chain gene. *Cell Motil. Cytoskeleton.* 17:301–308.

Rosenfeld, S.S., and B. Rener. 1994. The GPQ-rich segment of *Dictyostelium* myosin IB contains an actin binding site. *Biochemistry.* 33:2322–2328.

Sambrook, J., E.F. Fritsch, and T. Maniatis. 1989. Molecular Cloning: A Laboratory Manual. 2nd ed. Cold Spring Harbor Laboratory Press, Cold Spring Harbor, NY.

Sellers, J.R., and H.V. Goodson. 1995. Motor Proteins 2: myosins. Protein Profiles. 2:1323–1423.

Sikorski, R.S., and P. Hieter. 1989. A system of shuttle vectors and yeast host strains designed for efficient manipulation of DNA in *Saccharomyces cerevisiae. Genetics.* 122:19–27.

Silvadon, P., F. Bauer, M. Aigle, and M. Crouzet. 1995. Actin cytoskeleton and budding pattern are altered in the yeast rvs161 mutant: the Rvs161 protein shares common domains with the brain protein amphiphysin. *Mol. Gen. Genet.* 20:485–495.

Simon, V.R., T.C. Swayne, and L.A. Pon. 1995. Actin-dependent mitochondrial motility in mitotic yeast and cell-free systems: identification of a motor activity on the mitochondrial surface. *J Cell Biol.* 130:345–354.

Smith, M.G., V.R. Simon, H. O'Sullivan, and L.A. Pon. 1995. Organelle-cytoskeletal interactions: actin mutations inhibit meiosis-dependent mitochondrial rearrangement in the budding yeast *Saccharomyces cerevisiae. Mol. Biol. Cell.* 6:1381–1396.

Spudich, J.A., and H.M. Warrick. 1991. A tale of two motors. *Curr. Opin. Struc. Biol.* 1:264–269.

Stevens, B. 1977. Variation in number and volume of the mitochondria in yeast according to growth conditions. A study based on serial sectioning and computer graphics reconstruction. *Biol. Cell.* 28:37–56.

Titus, M.A., D. Wessels, J.A. Spudich, and D. Soll. 1993. The unconventional myosin encoded by the myoA gene plays a role in *Dictyostelium* motility. *Mol. Biol. Cell.* 4:233–246.

Ward, A.C. 1990. Single-step purification of shuttle vectors from yeast for high frequency back-transformation into *E. coli. Nucleic Acids Res.* 18:5319–5326.

Wessels, D., J. Murray, G. Jung, J. Hammer, and D.R. Soll. 1991. Myosin IB null mutants of *Dictyostelium* exhibit abnormalities in motility. *Cell Motil. Cytoskeleton.* 20(4):301–315.